

GT2017-64933

COMPARISON OF SUPERCRITICAL CO₂ POWER CYCLES TO STEAM RANKINE CYCLES IN COAL-FIRED APPLICATIONS

Jason D. Miller

Echogen Power Systems (DE), Inc.
Akron, Ohio, USA

David J. Buckmaster

Echogen Power Systems (DE), Inc.
Akron, Ohio, USA

Katherine Hart

Echogen Power Systems (DE), Inc.
Akron, Ohio, USA

Timothy J. Held

Echogen Power Systems (DE), Inc.
Akron, Ohio, USA

David Thimsen

Electric Power Research Institute
St. Paul, Minnesota, USA

Andrew Maxson

Electric Power Research Institute
Palo Alto, California, USA

Jeffrey N. Phillips

Electric Power Research Institute
Charlotte, North Carolina, USA

Scott Hume

Electric Power Research Institute
Charlotte, North Carolina, USA

ABSTRACT

Increasing the efficiency of coal-fired power plants is vital to reducing electricity costs and emissions. Power cycles employing supercritical carbon dioxide (sCO₂) as the working fluid have the potential to increase power cycle efficiency by 3 – 5% points over state-of-the-art oxy-combustion steam Rankine cycles operating under comparable conditions. To date, the majority of studies have focused on the integration and optimization of sCO₂ power cycles in waste heat, solar or nuclear applications. The goal of this study is to directly compare optimized cycle efficiencies of sCO₂ power cycles to state-of-the-art steam Rankine cycles using heat source and ambient characteristics of baseline oxy-fired coal plants.

This study is designed to demonstrate the potential of sCO₂ power cycles, and quantify the power cycle efficiency gains that can be achieved versus the state-of-the-art steam Rankine cycles employed in oxy-fired coal power plants. Turbine inlet conditions were varied among the sCO₂ test cases and compared with existing DOE/NETL steam base cases. Two separate sCO₂ test cases were considered and the associated flow sheets developed. The turbine inlet conditions for this study were chosen to match conditions in a coal-fired ultra-supercritical steam plant ($T_{inlet} = 593^{\circ}\text{C}$, $P_{inlet} = 24.1 \text{ MPa}$) and an advanced ultra-supercritical steam plant ($T_{inlet}=730^{\circ}\text{C}$, $P_{inlet} = 27.6 \text{ MPa}$). A plant size of 550 MW_e, was selected to match available information on existing DOE/NETL bases cases.

The effects of cycle architecture, combustion-air preheater temperature, and cooling source type were considered subject to comparable heat source and reference conditions taken from the steam Rankine reference cases. Combinations and variants of sCO₂ power cycles - including cascade and recompression and

variants with multiple reheat and compression steps - were considered with varying heat-rejection subsystems - air-cooled, direct cooling tower, and indirect-loop cooling tower. Where appropriate, combustion air preheater inlet temperature was also varied.

Through use of a multivariate nonlinear optimization design process that considers both performance and economic impacts, curves of minimum cost versus efficiency were generated for each sCO₂ test case and combination of architecture and operational choices. These curves indicate both peak theoretical efficiency and suggest practical limits based on incremental cost versus performance. For a given test case, results for individual architectural and operational options give insight to cost and performance improvements from step-changes in system complexity and design, allowing down selection of candidate architectures. Optimized designs for each test case were then selected based on practical efficiency limits within the remaining candidate architectures and compared to the relevant baseline steam plant. sCO₂ cycle flowsheets are presented for each optimized design.

NOMENCLATURE

| | |
|------|-----------------------------------|
| A | Heat Exchanger Surface Area |
| ACC | Air-Cooled Condenser |
| APHX | Air Preheater |
| ASU | Air Separation Unit |
| CPU | CO ₂ Purification Unit |
| DOE | Department of Energy |

| | |
|------------------|---------------------------------------|
| EPS | Echogen Power Systems (DE), Inc. |
| HHV | Higher Heating Value |
| HX | Heat Exchanger |
| LG | Low Grade Heat Recovery |
| NETL | National Energy Technology Laboratory |
| PCHE | Printed Circuit Heat Exchanger |
| PFHE | Plate and Frame Heat Exchanger |
| PHX | Primary Heat Exchanger |
| RC | Recompression |
| RHX | Recuperative Heat Exchangers |
| T | Temperature |
| TIT | Turbine Inlet Temperature |
| T-Q | Temperature - Enthalpy |
| U | Overall Heat Transfer Coefficient |
| WCC | Water-Cooled Condenser |
| c_p | Specific Heat |
| dT | Temperature Delta |
| sCO ₂ | Supercritical Carbon Dioxide |

INTRODUCTION

Increasing the efficiency of coal-fired power production is critical to reducing cost of electricity and minimizing associated emissions. sCO₂ power cycles have the potential to increase net plant efficiency by 3 to 5% points. Apart from gains in net plant efficiency, sCO₂ power cycles have the potential to offer advantages in lower operating and capital cost, physical plant size and the potential for water free operation. To date, most studies have focused on the integration of sCO₂ power cycles with concentrated solar power [1, 2, 3], nuclear [4, 5], and waste heat recovery [6] applications.

To establish a baseline that defines the potential gains in net plant efficiency, fully integrated flow sheets must be developed. The following defines important parameters that must be considered and their effects on the overall net plant efficiency.

MODELING AND OPTIMIZATION

Background

The theoretical performance of sCO₂ power cycles, as measured by thermodynamic efficiency, is generally calculated through steady-state modeling of the system under reasonable assumptions regarding component performance and loss mechanisms. While this approach provides an indication of the potential performance of a particular power cycle, it provides only limited insight into the effect of cycle architecture choice and neglects practical performance limits imposed by economic factors. Conventional iterative design becomes overwhelmed

very quickly given competing performance and economic demands in the face of dozens of degrees of freedom. Thus, traditional methods can suggest specific operational parameters (flow splits, pressure ratios, etc.) and equipment sizes (heat exchanger heat transfer [UA], turbine size, etc.) which are suboptimal to the overall plant design. To overcome this difficulty, Echogen Power Systems (DE), Inc. (EPS) has developed multivariate, nonlinear optimization software for design selection and evaluation of sCO₂ power cycles that is considerate of the multiple and competing metrics upon which such cycles are evaluated. The optimization software is MATLAB based, and makes use of several commercially available toolboxes along with internally developed cost and physical models of the plant components.

For an economic study on primary power cycles given a hard constraint on net power generation, one of the main metrics for evaluation of a candidate plant design is lifetime operating expense. For modern coal fired power plants, this expense is dominated by capital equipment and fuel cost. Within the power plant sub-scope of the power cycle, these metrics relate most strongly to heat exchanger cost and cycle efficiency. However, even given a power target and the seemingly straightforward desire to maximize cycle efficiency, incremental cost-versus-performance will asymptotically approach infinity as efficiency nears the cycle's theoretical limit; thus, the peak-efficiency design will not be the optimal design when capital costs are considered. To quantify these competing influences, EPS tools were used to extract a family of fixed-output, minimal-cost designs that span the achievable efficiency range. This continuum of cost-optimal designs revealed the relationship between power-cycle capital expenditure and system performance, and allows informed decision-making on the point of diminishing returns subject to external constraints such as net power produced, heating or cooling sources or cost.

Steam Baseline Cases and Comparison Metrics

The steam cycles with which the sCO₂ Brayton power cycles discussed here are compared are based on those published by DOE/NETL [1]. These are straightforward single reheat steam cycles with steam turbine-driven feedwater pumps. Low-temperature cycle condensate is used to cool the main air compressor in the air separation unit and product CO₂ compressor in the CO₂ purification unit. The heat absorbed by the condensate reduces the LP steam extraction for feedwater heating. Recovery of this lower temperature heat has not been incorporated into the sCO₂ Brayton power cycles discussed here, although there is some potential benefit in incorporating these heat sources. Important characteristics of the steam systems are summarized TABLE 1.

The sCO₂ turbine inlet conditions for test case one were chosen to match exactly to those in DOE/NETL reference case S12F. The published turbine inlet conditions for the DOE/NETL reference case S13F are 649°C/649°C/27.5 MPa, somewhat lower than is otherwise anticipated for ultra-supercritical steam cycles. For test case two, steam base case

turbine inlet conditions were chosen to match what is considered to be the maximum achievable today: 730°C/760°C/27.6 MPa.

Performance of the reference case, S13F was recalculated to incorporate the higher turbine inlet temperatures. The overall arrangement of the S13F steam cycle was unchanged including feedwater heater pressures, condensate/steam extractions to heating/cooling loads outside the steam cycle and condensate return from these heating/cooling loads. The primary effect of this steam cycle recalculation is an incremental reduction in main steam flow (for the same net plant output) and a corresponding reduction in fuel flow to the steam generator. The reduction in fuel flow also incrementally reduces power use in fans supporting boiler operation and the ASU/CPU. The net plant efficiency incorporating the recalculated steam and fuel flow resulted in a net plant efficiency rise of 32.6 to 35% with respect to the higher heating value (HHV).

TABLE 1 SUMMARY OF STEAM BASE CASES.

| | S12F | S13F (modified) |
|--|-------------|------------------------|
| Turbine Inlet Pressure (MPa) | 24.1 | 27.6 |
| Turbine Inlet Temperature (°C) | 593 | 649 (730*) |
| Gross Electrical Output (MW _e) | 748.3 | 741.7 |
| Dry Bulb Temperature (°C) | 5.6 | |
| Wet Bulb Temperature (°C) | 2.8 | |
| Barometric Pressure (bar) | 0.9 | |
| Net Electrical Output (MW _e) | 550 | 550 |
| Thermal Input, HHV (GW _{th}) | 1.76 | 1.69 |
| Net Plant Efficiency, HHV (%) | 31.2 | 32.6 (35*) |

*Numbers adjusted from reference case.

The detailed parasitic load list, shown in TABLE 2, from the DOE/NETL report for each reference case were analyzed for apparent scaling relationships to either the higher heating value (HHV) heat input or gross generator output. Burner-related loads (e.g. coal conveyance/processing, combustion air movement, CO₂ capture systems, etc.) scale well with HHV heat input, while transformer losses scale with gross generation. Other miscellaneous component auxiliaries and balance of plant loads were taken as constants. The aggregate of this analysis is shown the scaling rules used for sCO₂ test cases in TABLE 2, and was used to anticipate full plant auxiliary loads for the two sCO₂ power cycle test cases. For all cases the generator efficiency was assumed to be 99.5%. [5]

Finally, steam and sCO₂ systems were compared on the basis of net plant efficiency with respect to the HHV heat input. This is defined as the ratio of net electrical power output to the HHV coal heat input. The net plant efficiency for the steam reference cases is explicitly stated by DOE/NETL, as noted in [7], and summarized in TABLE 1. For the sCO₂ systems, an overall burner-system efficiency of 88.3% was assumed based

on analysis of NETL documents and input from industry partners.

Trade Studies

Cycle Architectures

For each test case, a variety of potential sCO₂ power cycle architectures were considered ranging in complexity from a cascade-like layout to variants of a standard recompression cycle combined with a reheat turbine and multiple compression stages.

TABLE 2 INCLUDED AUXILIARY LOADS

| Auxiliary Load | Reference Loss (kW_e) | Scaling rules used for sCO₂ test cases |
|-------------------------|--|---|
| Coal Handling | 570 | Loads scaled with thermal input (178.5 MW _e for 1.76GW _{th}) |
| Pulverizers | 4770 | |
| Sorbent/Reagent | 180 | |
| Ash Handling | 1070 | |
| Primary Air Fans | 2240 | |
| Forced Draft Fans | 880 | |
| Induced Draft Fans | 7280 | |
| Main Air Compressor | 93710 | |
| Baghouse | 150 | |
| Spray Dryer FGD | 2910 | |
| CPU | 64740 | Loads held constant (3.4 MW _e) |
| ASU aux | 1000 | |
| Misc BOP | 2000 | |
| Steam Turbine Aux | 400 | Values estimated from EPS performance models |
| Condensate Pumps | 990 | |
| Circulating Water Pumps | 3280 | |
| Ground Water Pumps | 320 | |
| Cooling Tower Fans | 2110 | |
| ACC Fans | 6910 | |
| Transformer Losses | 2780 | Loads scaled with gross generator output (748.3 MW _e) |

The cascade cycle variant examined here, and shown in FIGURE 1, is the EPS dual-rail architecture which maintains the cascade cycle’s general tendency towards heat absorption over a large source-temperature range, and provides additional flexibility for mixing flow between recuperators (RHX1 and RHX2) and lower-grade primary heat exchangers (PHX2-3) to better match the overall system temperature enthalpy (T-Q) curve [6]

The baseline recompression (RC) cycle sees the addition of a high-temperature compressor, but contains only a single PHX. The flow diagram for this architecture is shown in FIGURE 2. A major strength of the recompression cycle is that its heat absorption occurs over a limited source temperature range. From a Carnot perspective, this serves to raise the average hot source temperature, and with it the maximum achievable power cycle efficiency. Additionally, the high-temperature compressor serves to avoid heat rejection beyond what is possible through recuperation.

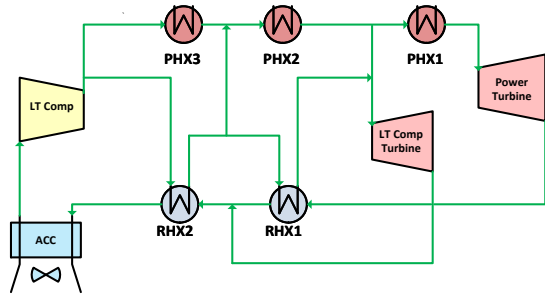


FIGURE 1 CASCADE CYCLE

An important consideration in these studies is the effect of the heat source temperature leaving the power-cycle (exhaust gas from the lowest temperature PHX). This exhaust has thermal resources that can still be exploited. It is used to feed the heat source side air preheater, which preheats the oxygen feeding the combustion process. Generally, heat recovered by the air preheater results in less fuel burn. An upper limit on this temperature, due to temperature limits placed on the heat source air preheater (APHX), is a hindrance to the RC cycle. This limit places an explicit constraint on the high-pressure side outlet temperature of the high-temperature recuperative heat exchanger (RHX1) limiting the amount of recuperation that can be achieved. This effect can be mitigated either by pushing the heat source-side APHX to higher inlet temperatures or with the addition of low-grade PHX sections to the baseline recompression cycle (RC-LG), effectively merging it with the cascade architecture. This hybrid cycle, recompression with low grade heat recovery (RC-LG), is shown in FIGURE 3.

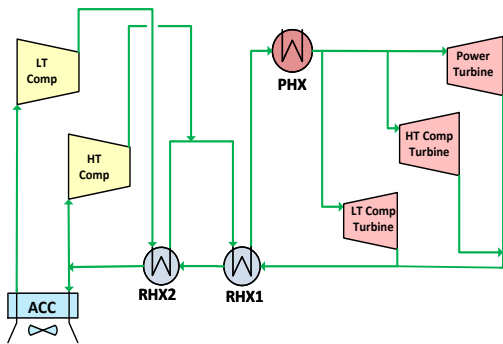


FIGURE 2 BASELINE RECOMPRESSION CYCLE

The addition of a reheat-stage is straightforward modification to the RC-LG cycle. The effect of a reheat stage alone tends to be less significant for $s\text{CO}_2$ cycles than for steam—the required inlet pressure of the low-temperature compressor ($P_{\text{sat}}(T_{\text{amb}})$) in an $s\text{CO}_2$ cycle has a much higher floor than the analogous state in an advanced steam cycle. This is due to CO_2 's less favorable saturation line. For this reason, the theoretical benefits of reheat are frequently limited by an $s\text{CO}_2$ cycle's lower expansion ratio. This expansion ratio can be grown with the addition of a "series compression" stage after the low-

pressure outlet of the low-temperature recuperative heat exchanger (RHX2), but this comes at the expense of additional compression work. An additional RHX is added at the series-compressor discharge to maximize internal recuperation. The cycle is shown FIGURE 4.

In all cases, a shaft-coupled drive turbine exists for each compression component, and plant output is provided by a single generator.

Cooling Subsystem

Although water-cooled steam condensers with wet cooling towers are the common practice, regulatory requirements and water scarcity in many locations have led to increased interest in dry-cooling systems [8]. Water-cooled systems (without intermediate loops) benefit from their ability to approach the ambient wet-bulb temperature. But this benefit comes with significant cost in the form of additional parasitic loads and operating costs arising from the required makeup water in cooling tower systems. Additionally, PCHE manufacturers advise operating water-cooled condensers only in closed (clean) water loops [9]. For a water-cooled $s\text{CO}_2$ system, then, the wet-bulb benefit is undercut by an additional approach within an intermediate heat exchanger. A detailed review of the impacts of wet versus dry cooling on $s\text{CO}_2$ is presented in [10].

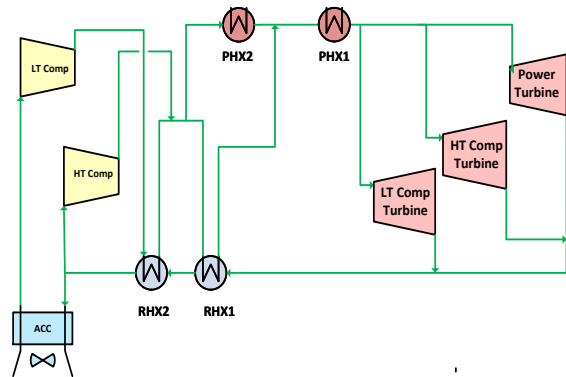


FIGURE 3 BASELINE RECOMPRESSION CYCLE WITH LOW GRADE HEAT RECOVERY

Air Preheater Temperature

As discussed in the architecture description above, constraints on the temperature of the thermal resources exiting the power cycle have a major impact on the baseline RC cycle efficiency. At the onset of this study, it was assumed that the coal combustion products would need to be cooled to a maximum value of 371°C , a gas temperature commonly leaving the economizer in a steam generator and a maximum gas inlet temperature for commercial APHX. Given the expectation that a RC cycle should have theoretically higher performance than any cascade option, it was necessary in this study both to quantify the performance impact to the RC cycle of capping internal recuperation and to identify potential performance benefits from operating these components at more aggressive temperatures.

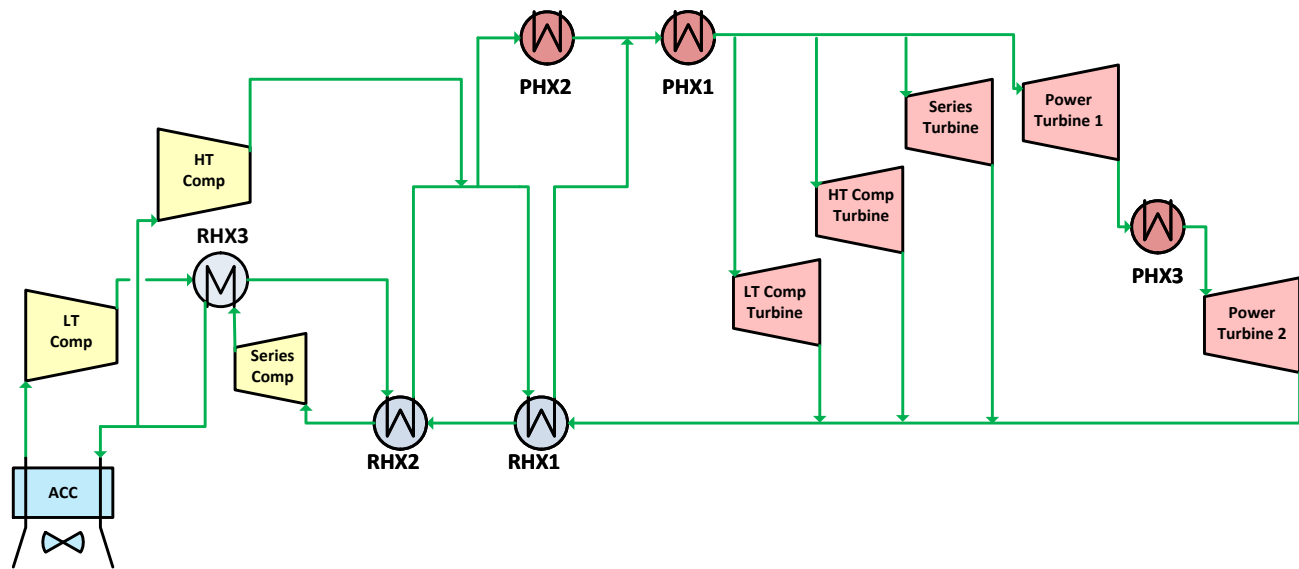


FIGURE 4 BASELINE RECOMPRESSION WITH LOW GRADE HEAT RECOVERY, SERIES COMPRESSION AND REHEAT

Performance Models

Physical performance models for each of the main power cycle components were developed and implemented within the EPS cycle optimization software. Generally, heat exchangers operate with freedom on thermal size or UA (based on a discretized log-mean temperature difference), but are subject to limiting performance constraints on pressure-drops and overall effectiveness. The limits are based experience as detailed in the following section. Compressors and turbines operate with a constraining relationship between efficiency and size (shaft power) [6], with the overriding assumption being that smaller pieces of turbomachinery are inherently less efficient.

The system is permitted to operate sub-critically, and in such cases, the low temperature compression components respect a 0.69MPa adiabatic suction margin with respect to the low temperature compressor inlet enthalpy at saturation. Internal minor flow losses such as hydrostatic bearing supply flows and seal leakages are approximated by artificially deflating component efficiencies. Internal piping losses are neglected for this study.

Heat Exchanger Performance

System RHXs and water-cooled condensers (WCCs) are assumed to be PCHEs that achieve high performance relative to other design types [11]. Both the high and low pressure side pressure drops within RHXs are treated as independent free variables, but limited to a minimum value of 0.1MPa. WCC CO_2 - and water-side pressure drops are fixed at 0.25MPa. PCHE thermal effectiveness is constrained to a maximum of 98%.

Cooling tower performance modeling is based on the generally accepted theory developed by Merkel [12, 13]. An empirical model relates overall cooling tower performance to

water and air mass fluxes, and the water approach to the ambient wet-bulb temperature is limited to approximately 4.2°C [14]. For indirect cooling tower systems, the intermediate heat exchanger is taken to be a plate and frame type (PFHE) with its effectiveness limited to 90% and pressure drops fixed at 0.1MPa.

Air-cooled condensers (ACCs) are modeled with a fixed CO_2 -side pressure drop of 0.1MPa, and an empirically derived linear relationship between UA and fan parasitic load based on observed vendor performance quotes is enforced.

Primary heater blocks (PHXs) were modeled with fixed pressure drops of 0.69MPa per heat exchanger section and constrained to a minimal endpoint approach of 27.8°C based on preliminary input from industry partners. The relationship between absorbed heat and source temperature was enforced through integration of T-Q diagrams from reference plants.

Cost Models

Because, in coal-fired applications, the sCO_2 power cycle represents a limited fraction of the overall plant cost, a complete economic optimization of the plant cannot be achieved by optimizing the power cycle alone. However, it is reasonable to expect that outside of the power cycle itself, costs should generally be negatively correlated to overall plant efficiency; i.e. given a design-requirement on net plant output, capital expense of source-side components should increase with required thermal input (e.g., increase with lower power cycle efficiency). This, combined with the general economic desire to minimize lifetime fuel input, makes it reasonable to restrict the cost “scope” early in the design process to the power cycle alone.

Within the power cycle, costs are dominated by heat exchangers and turbomachinery. For cases of fixed cycle

architecture (number of pieces of rotating equipment) and desired output, it is expected that variability in turbomachinery capital expenditure versus cycle performance will be dominated by much larger changes in the cost of the heat exchangers. Based on this turbomachinery is assumed to contribute a nominally fixed capital cost, and given the primary interest in this study is in incremental cost, is neglected. When comparing systems with different architectures which result in a step-change in turbomachinery complexity (e.g. the “cascade” and “recompression” cycles), one must be mindful of the (hidden) step-change in predicted cost. However, the discrete choice of a power cycle architecture is more likely to be made on the basis of significant changes to performance or operational complexity rather than on incremental cost. Similarly, other cycle costs such as piping and valving, control systems, etc. are treated as nominally fixed and neglected.

EPS experience is that the expense of a given heat exchanger is strongly correlated to the unit’s dry mass. Further, qualitative relationships between HX mass and certain HX fluid/thermal characteristics are easily predictable. For example, physical size should have a positive relationship to “thermal size” (UA) and a negative relationship to fluid pressure drops. Based on an internal database of vendor quotes over a wide range of operating conditions and heat exchanger types, proprietary relationships between HX fluid and thermal characteristics for consistent sets of heat exchanger type and material have been developed to predict unit costs as a function of fluid and thermal characteristics (namely flow rates, UA, and pressure drops). For the largely-unconstrained RHXs, a full-order cost model is used. For other, more highly constrained HX types, reduced-order (UA only) models are used.

Finally, cooling tower costs (when present) are predicted using Zanker’s correlation, adjusted to present-day dollars [13].

RESULTS AND DISCUSSION

Effect of Cycle Architecture

The selection of cycle architecture has a significant impact on the potential net cycle efficiency. As previously discussed, this study considered cascade, recompression (RC) and variants of the recompression cycle—RC with low-grade heat recovery (RC-LG), RC-LG with series compression, and RC-LG with both series compression and turbine reheat. Recall that the tracked cost only includes the power cycle heat exchangers and cooling sink (RHX, WCC, ACC, cooling tower). This is important to note when comparing cycle architectures with varying numbers of turbomachinery as we are here. If the additional turbomachinery costs would be included in the analysis, it is expected that the cost index for RC-LG with series compression and both series compression and turbine reheat would be offset up by a fixed amount. This would correspond to the discrete cost of the additional turbomachinery.

FIGURE 5 and FIGURE 6 summarize the impact of the selection of cycle architecture on the net plant efficiency and plant cost with turbine inlet temperatures of 593°C and 730°C

respectively. Significantly, cascade cycles perform poorly in both applications even when compared to the baseline RC cycle. The theoretical maximum achievable efficiency for the cascade cycles were 27% and 32% for turbine inlet temperatures of 593°C and 730°C respectively. This does not compare well against the base line RC efficiencies of 34% and 34.5% for the same turbine inlet temperatures. The performance deficit of the cascade cycles in this type of application (recirculated heat source) has been discussed in literature: cascade cycles are designed to minimize the unrecovered enthalpy in the heat source and achieve high thermodynamic efficiency [6]. For applications in which the heat source is circulated, this fundamental trait of cascade cycles will result in lower conversion efficiency and therefore a lower potential net plant efficiency.

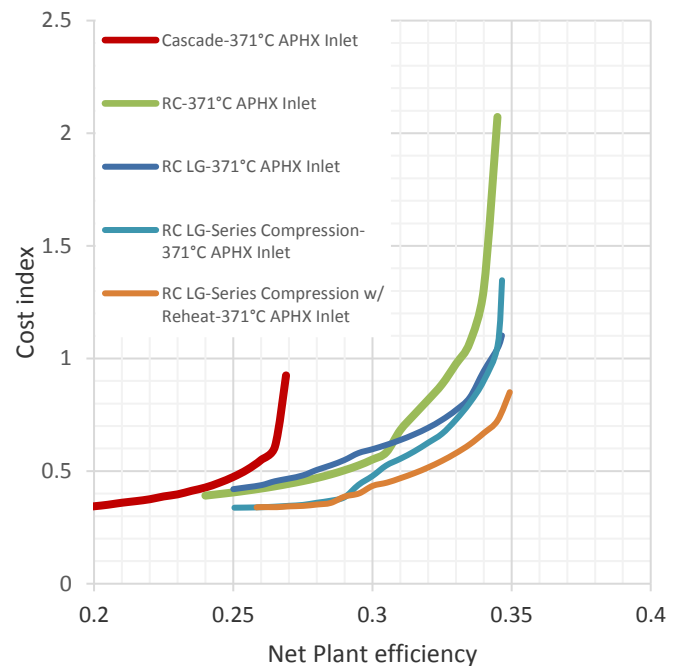


FIGURE 5 EFFECT OF CYCLE SELECTION TIT 593°C

While the results indicate the RC cycle easily outperforms cascade cycles in this application. There are still gains to be made if one considers variants of the recompression cycle. As discussed previously, the addition of either a high temperature air preheater (APHX inlet temperature greater than 371°C) or a low temperature primary heater coil can increase net plant efficiency for a 593°C turbine inlet temperature by 0.5% points and for a 730°C turbine inlet temperature net plant efficiency increases by 5.0% points. The higher temperature cases benefitting more due to the higher amounts of recuperation that can be achieved if the external constraints (due to APHX temperature limits) are removed.

The results showed no benefit to adding series compression and an approximate 1% point increase in net plant efficiency if both series compression and a turbine reheat path is utilized.

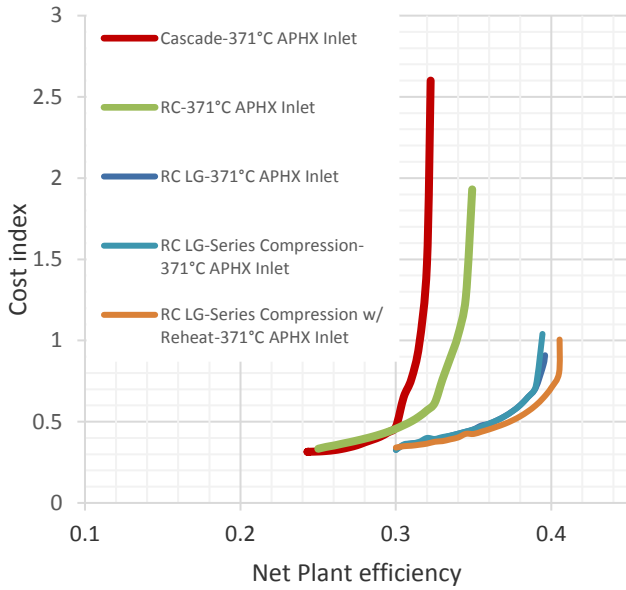


FIGURE 6 EFFECT OF CYCLE ARCHITECTURE TIT 730°C
Effect of Combustion Air Preheater Inlet Temperature

The effect of APHX inlet temperature (temperature to which the power cycle cools the primary heat flow) was considered for the baseline recompression cycle depicted in FIGURE 2. A plant size of 550 MW_e net with a turbine inlet temperature of 593°C and a 27.8°C approach between the CO₂ inlet temperature and the PHX exhaust temperature was assumed to study the effect of APHX inlet temperature on net plant efficiency. APHX inlet temperatures of 371°C, 426°C and 482°C were considered. Results in FIGURE 7 show that the positive effect of APHX inlet temperature is limited to 426°C; moving above this neither increases net plant efficiency nor decreases tracked cost. At 426°C, recuperation is now limited by the turbine discharge temperature (not APHX inlet temperature) and model constraints placed on the high temperature recuperative heat exchanger (RHX1). FIGURE 8 attempts to illustrate this point. A low APHX temperature combined with the minimal PHX approach effectively limits the final RHX1 outlet temperature. At the point where efficiency gains are no longer observed, the limit at that state has shifted to be defined by the turbine discharge temperature.

It should be noted here, that the primary burner efficiency was considered constant for this study. The APHX inlet temperature will have an indirect effect on the primary burner efficiency that was not captured in these results. Based on published curves [15, 16] showing boiler efficiency gain versus reduction in flue gas temperature it is expected that for a 27.7°C increase in APHX inlet temperature, there is corresponding increase of 55.5°C in flue gas exit temperature, resulting in approximately a 1.0% decrease in primary burner efficiency. This is important to note as one must weigh the potential benefit

of raising the APHX inlet temperature versus the reduction in heater efficiency that will follow.

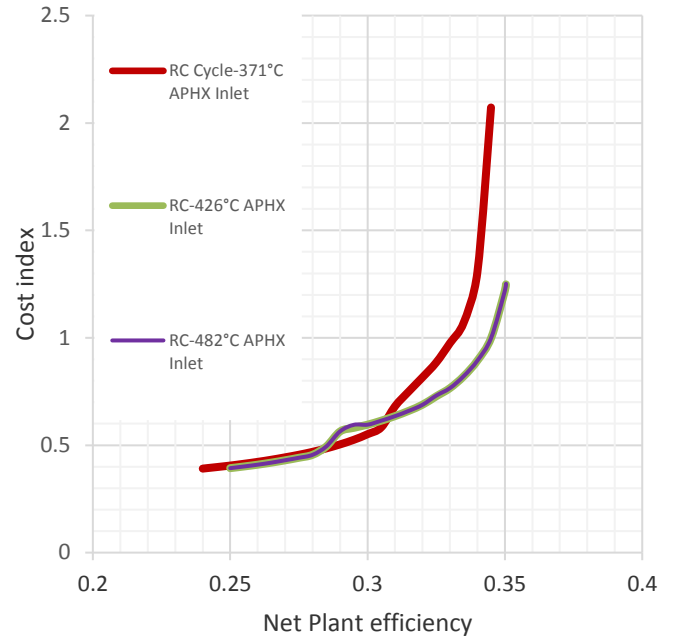


FIGURE 7 EFFECT OF APHX INLET TEMPERATURE RC CYCLE TIT 593°C

If one considers the addition of a low-grade heat recovery section in the PHX, as shown in FIGURE 3, similar increases in net plant efficiency can also be realized. A low-grade primary coil (PHX2) is added in parallel with the power cycle recuperators (RHX1, 2) with potential flow split and mixing in between. Only a small portion of the power cycle flow (approximately 10%) is diverted to PHX2 with the rest passing through the high temperature recuperative heat exchanger (RHX1). The flow is then mixed at the discharge of PHX2 and sent to the high temperature primary heater (PHX1) and finally to the power and drive turbines. This simple yet significant change in the cycle architecture allows for a more efficient use of the high temperature recuperative heat exchanger (RHX1). Heat still available after the turbine work has been extracted can be better utilized because RHX1 discharge temperature is no longer limited by the APHX inlet temperature (plus the required approach), but only to the turbine discharge temperature. Results of this can be seen in FIGURE 9. For a standard RC cycle with a 593°C turbine inlet temperature and 371°C APHX inlet temperature (RC 371°C APHX Inlet), the maximum achievable theoretical net plant efficiency is 34.5% HHV. An additional 0.5% is available if a high temperature APHX or some low-grade heat recovery is utilized, and at efficiencies where the architectures overlap, costs are significantly lower. To achieve 34.5% HHV net plant efficiency for a standard recompression cycle, a cost index of 2.1 is required. The same efficiency may be achieved utilizing either low-grade heat recovery or a high temperature APHX with a cost index of 1.

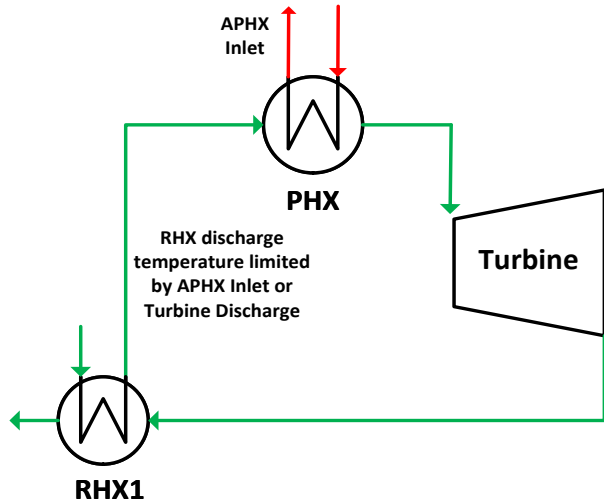


FIGURE 8 RECOMPRESSION CYCLE HEAT EXCHANGER ARRANGEMENT

This result is more pronounced for systems with higher turbine inlet temperatures. FIGURE 10 shows that for turbine inlet temperature of 730°C, the maximum theoretical efficiency for a baseline RC cycle with an APHX inlet temperature of 371°C is 35% HHV. With the addition of a high temperature APHX or low-grade heat recovery, the maximum theoretical net plant efficiency approaches 40%. If a high temperature APXH is utilized, it would have to be capable of operation to 593°C (outside today's state-of-the-art) to achieve these high efficiencies. Alternatively, a commercially available APHX operating at 371°C can be used along with a recompression cycle utilizing a low-grade heat recovery section in the primary heater (PHX2) to achieve net plant efficiencies approaching 40% HHV.

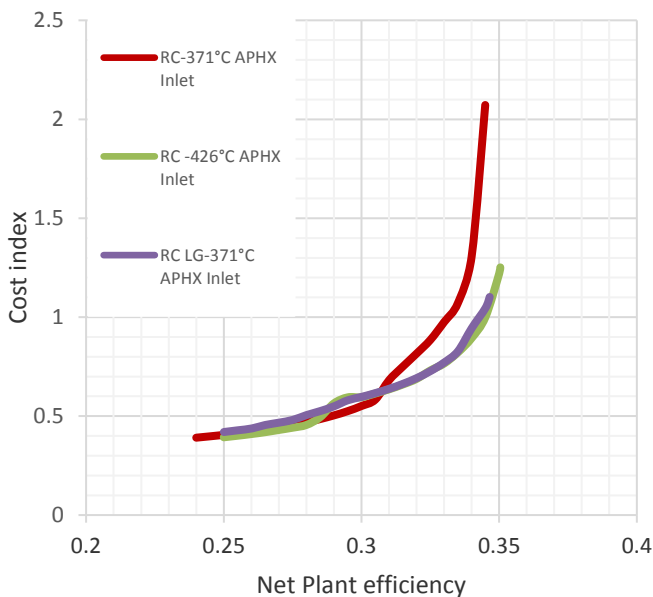


FIGURE 9 EFFECT OF LOW-GRADE HEAT ADDITION RECOMPRESSION CYCLE TIT - 593°C

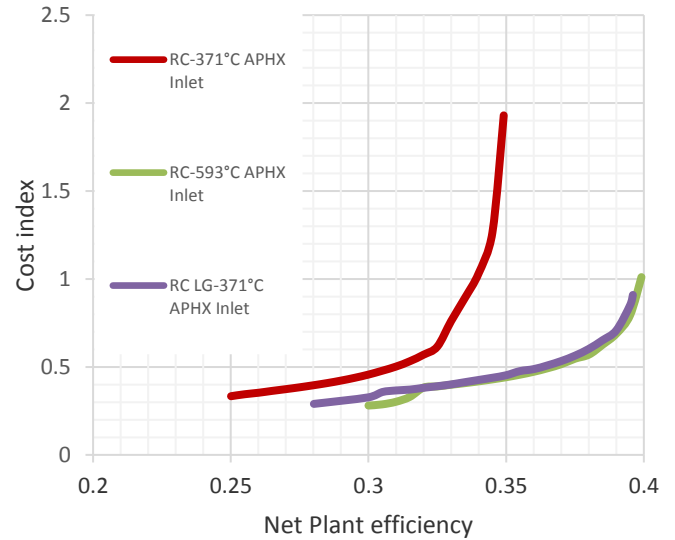


FIGURE 10 EFFECT OF LOW-GRADE HEAT ADDITION RECOMPRESSION CYCLE TIT - 730°C

Effects of Cooling Sink Selection

Performance of a baseline recompression system with 593°C turbine inlet temperature and 371°C APHX inlet temperature was considered for three heat rejection schemes. Direct CO₂ to air using an ACC, direct CO₂ to cooling tower water through a single WCC, and indirect CO₂ to cooling tower water with an intermediate clean water loop. Results are summarized in FIGURE 11, and direct WCC cooling has an incremental performance advantage over the air and indirect water cooling. These advantages in cost and potential net plant efficiency are not achievable today in direct water cooling systems as there are practical limitations of PCHEs and the very small channel size utilized in their design. These practical limitations preclude the use of direct cooling in practice, but the authors wished to show the potential gains. Results also show that air cooled heat rejection systems perform better than indirect water cooled systems. Indirect water cooling schemes require two heat exchangers, and therefore three temperature approaches—one between the wet bulb temperature and the cooling tower water, and one each between the cooling tower water, clean water, and CO₂. Because of this added approach to the wet bulb temperature and additional pumping parasitic, potential advantages in efficiency and cost from water cooling are lost.

SUMMARY

Two 550 MW_e net power sCO₂ power cycles for integration with an oxy-fired coal plant were developed using a nonlinear, multivariate cycle optimization design process. Parameters investigated were APHX inlet temperature, turbine inlet conditions, cycle architecture, and heat rejection scheme. Results of the architecture study indicate the recompression cycle and its variants as the preferred cycle architecture for this application, outperforming cascade cycles. It was also shown that recompression cycle performance is heavily dependent on

air preheater inlet temperature with potential efficiency gains of 0.5% to 5.0% points as it is increased. The study on heat rejection showed that for the sCO₂ power cycles studied, direct CO₂ to air cooling using an ACC is the preferred option, as direct water cooling is not a viable option for PCHes.

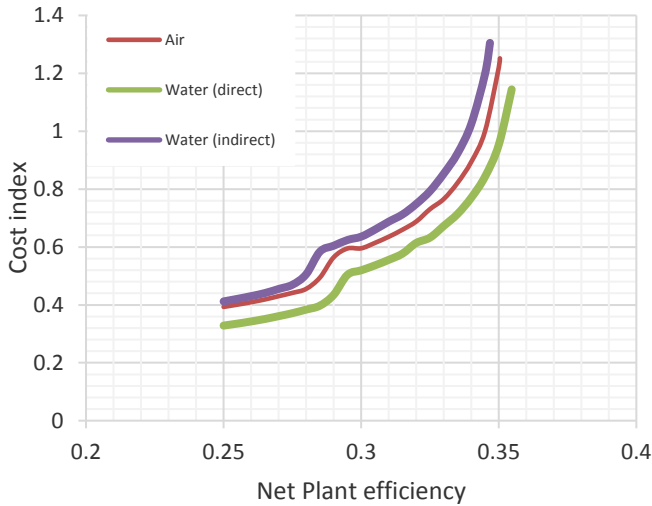


FIGURE 11 EFFECT OF HEAT REJECTION SCHEME- TURBINE INLET TEMP. 593°C

Flow sheets for turbine inlet temperatures of 593°C (Test Case 1) and 730°C (Test Case 2) are shown in Annex A and B respectively. Test Case 1 is a baseline recompression cycle, with an APHX inlet temperature of 427°C. Test Case 2 is a baseline RC cycle with low grade heat recovery (RC-LG). The air preheater inlet temperature is 371°C. Direct CO₂ to air cooling was chosen for each of the flow sheets. Results of the optimization compared well against the state of the art steam cycles pulled from the DOE/NETL reference cases S12F and S13F. FIGURE 12 summarizes the cycle comparison. It shows the potential net efficiency gains of 3.3% for turbine inlet temperatures of 593°C and net efficiency gains of 4% for turbine inlet temperatures of 730°C.

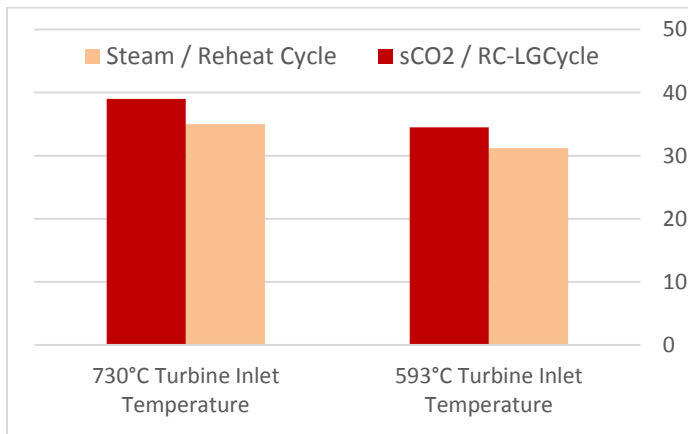


FIGURE 12 DOE/NETL REFERENCE CASE TO sCO₂ POWER CYCLE NET PLANT EFFICIENCY COMPARISON

ACKNOWLEDGMENTS

The work presented here was funded by the U.S. DOE/NETL under agreement DE-FE0025959.

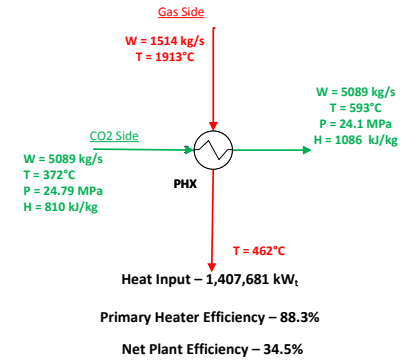
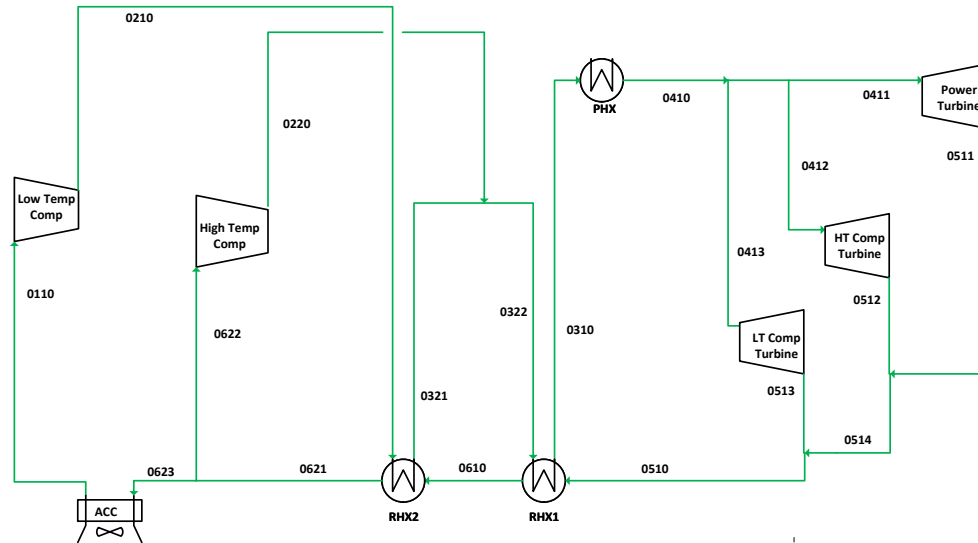
REFERENCES

- [1] T. Neises and C. Turchi, "Supercritical CO₂ Power Cycles: Design Considerations for Concentrating Solar Power," in *The 4th International Symposium - Supercritical CO₂ Power Cycles*, 2013.
- [2] T. Neises and C. Turchi, "A Comparison of Supercritical Carbon Dioxide Power Cycle Configurations with an Emphasis on CSP Applications," *Energy Procedia*, vol. 49, pp. 1187-1196, 2014.
- [3] M. A. Reyes-Belmonte, A. Sebastian, M. Romero and J. Gonzalez-Aguilar, "Optimization of a Recompression Supercritical Carbon Dioxide Cycle for an Innovative Central Receiver Solar Power Plant," *Energy*, vol. 112, pp. 17-27, 2016.
- [4] J. J. Sienicki, A. Moissevtey and L. Krajtl, "Utilization of the Supercritical CO₂ Brayton Cycle With Sodium-Cooled Fast Reactors," in *The 4th International Symposium - Supercritical CO₂ Power Cycles*, 2014.
- [5] V. Dostal, P. Driscoll and P. Hejzlar, *A Supercritical Carbon Dioxide Cycle for Next Generation Nuclear Reactors*, 2004.
- [6] T. Held, "Supercritical CO₂ cycles for gas turbine combined cycle power plants," in *Power Gen International*, 2015.
- [7] DOE/NETL-401/093010, "Cost and Performance of Low-Rank Pulverized Coal Oxycombustion Energy Plants: Final Report," 2010.
- [8] J. N. Phillips, "Cooling Requirements and Water Use Impacts of Advanced Coal-fired Power Plants with CO₂," Electric Power Research Institute, Palo Alto, CA, 2010.
- [9] Heatric, "Heat Exchanger User's Manual. Installation, Operation & Maintenance Instructions for Heatric Printed Circuit Heat Exchangers (PCHes), Formed Plate Heat Exchangers (FPHEs) and Hybrid Heat Exchangers (H2X)," 2015.
- [10] T. Held, J. Miller and D. Buckmaster, "A Comparative Study of Heat Rejection Systems for sCO₂ Power Cycles," in *The 5th International Supercritical CO₂ Power Cycles Symposium*, 2016.
- [11] R. L. Pierres, D. Southall and S. Osborne, "Impact of Mechanical Design Issues on Printed Circuit Heat Exchangers," in *Proceedings of sCO₂ Power Cycle Symposium*, Boulder, Colorado, 2011.
- [12] H. B. Nottage, "Merkel's Cooling Diagram as a Performance Correlation for Air-Water Evaporative Cooling Systems," *ASHVE Transactions*, vol. 47, p. 429, 1941.

- [13] S. A. Leeper, "Wet Cooling Towers: Rule-of-Thumb Design and Simulation," US Department of Energy, Idaho National Engineering Laboratory, 1981.
- [14] J. Hensley, Cooling Tower Fundamentals, Marley Cooling Tower Company, 2009.
- [15] J. B. K. a. S. C. Stultz, "Economizers and Air Heaters," in *Steam, Its Generation and Use Vol. 41*, Barberton, The Babcock & Wilcox Company, 2005, pp. 20-1.
- [16] R. Pachaiyappan and j. D. Prakash, "Improving the Boiler Efficiency by Optimizing the Combustion Air," *Applied Mechanics and Materials*, vol. 787, pp. 238-242, 2015.

ANNEX A

550 MWE sCO₂ POWER CYCLE FLOW SHEET – 593°C TURBINE INLET TEMPERATURE



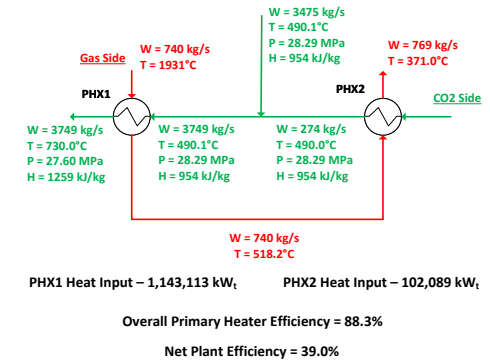
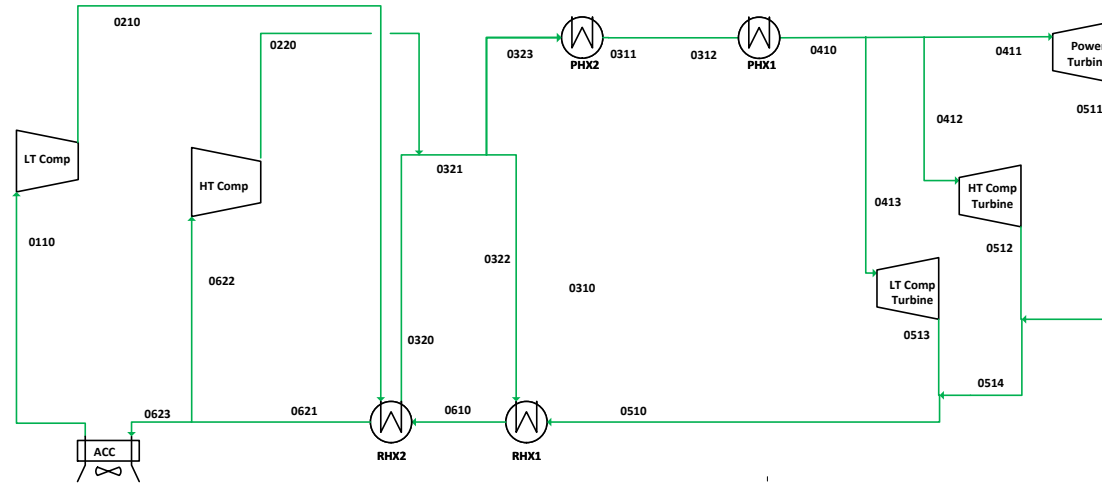
| State | Description | Temperature (°C) | Pressure (MPa) | Flow (kg/s) | Enthalpy (kJ/kg) |
|-------|--|------------------|----------------|-------------|------------------|
| 0110 | ACC Outlet - LT Comp Inlet | 11.7 | 5.33 | 2840 | 229 |
| 0210 | LT Comp Outlet - RHX2 HP Inlet | 31.2 | 26.32 | 2840 | 254 |
| 0220 | HT Comp Outlet | 181.6 | 25.16 | 2249 | 555 |
| 0321 | RHX2 HP Outlet | 183.2 | 25.16 | 2840 | 557 |
| 0322 | RHX1 HP Inlet | 182.5 | 25.16 | 5089 | 556 |
| 0310 | RHX1 HP Outlet - PHX Inlet | 372 | 24.79 | 5089 | 810 |
| 0410 | PHX Outlet | 593 | 24.1 | 5089 | 1086 |
| 0411 | Power Turbine Inlet | 593 | 24.1 | 3690 | 1086 |
| 0412 | HT Comp Turbine Inlet | 593 | 24.1 | 1026 | 1086 |
| 0413 | LT Comp Turbine Inlet | 593 | 24.1 | 373 | 1086 |
| 0511 | Power Turbine Outlet | 413.8 | 5.68 | 3690 | 887 |
| 0512 | HT Comp Turbine Outlet | 417.4 | 5.68 | 1026 | 891 |
| 0513 | LT Comp Turbine Outlet | 421.1 | 5.68 | 373 | 895 |
| 0514 | LT Comp Turbine + Power Turbine Outlet | 414.7 | 5.68 | 4716 | 888 |
| 0510 | RHX1 LP Inlet | 415 | 5.68 | 5089 | 889 |
| 0610 | RHX1 LP Outlet - RHX2 LP Inlet | 187.3 | 5.58 | 5089 | 635 |
| 0621 | RHX2 LP Outlet | 43.4 | 5.48 | 5089 | 465 |
| 0622 | HT Comp Inlet | 43.4 | 5.48 | 2249 | 465 |
| 0623 | ACC Inlet | 43.4 | 5.48 | 2840 | 465 |

| SYSTEM PARASITICS | Loss (kW _e) | Power (kW _e) |
|---------------------------|-------------------------|--------------------------|
| Power Turbine Gross Power | | 736,233 |
| Gearbox/Generator | (3,681) | |
| Component Electrical | (15,590) | |
| Coal Handling | (516) | |
| Pulverizers | (4,316) | |
| Sorbent / Reagent | (163) | |
| Ash Handling | (968) | |
| Primary Air Fans | (2,027) | |
| Forced Draft Fans | (796) | |
| Induced Draft Fans | (6,587) | |
| Main Air Compressor | (84,791) | |
| ASU Aux | (1,000) | |
| Baghouse | (136) | |
| Spray Dryer FGD | (2,633) | |
| CPU | (58,578) | |
| Misc BOP | (2,000) | |
| Turbine Aux | (400) | |
| Transformer Losses | (2,051) | |
| System Net Power | | 550,000 |

| Component | Duty (kW) |
|-----------------------------------|-----------|
| LT Turbo-Compressor - Shaft Power | 71,305 |
| HT Turbo-Compressor - Shaft Power | 200,464 |
| Power Turbine - Shaft Power | 736,233 |
| ACC - Heat Transferred | 671,449 |
| RHX1 - Heat Transferred | 1,290,853 |
| RHX2 - Heat Transferred | 860,538 |
| PHX - Heat Transferred | 1,407,681 |

ANNEX B

550 MWE sCO₂ POWER CYCLE FLOW SHEET – 730°C TURBINE INLET TEMPERATURE



| State | Description | Temperature (°C) | Pressure (MPa) | Flow (kg/s) | Enthalpy (kJ/kg) |
|-------|--|------------------|----------------|-------------|------------------|
| 0110 | ACC Outlet - LT Comp Inlet | 12.4 | 5.4 | 2206.0 | 231 |
| 0210 | LT Comp Outlet - RHX2 HP Inlet | 35.5 | 30.5 | 2206.0 | 261 |
| 0220 | HT Comp Outlet | 202.2 | 29.0 | 1543.2 | 576 |
| 0320 | RHX2 HP Outlet | 208.9 | 29.0 | 2206.0 | 586 |
| 0321 | RHX2 HP Outlet +HT Comp Outlet | 206.1 | 29.0 | 3749.2 | 582 |
| 0322 | RHX1 HP Inlet | 206.2 | 29.0 | 3475.2 | 582 |
| 0323 | PHX2 Inlet | 206.1 | 29.0 | 274.1 | 582 |
| 0310 | RHX1 HP Outlet | 490.1 | 28.3 | 3475.2 | 954 |
| 0311 | PHX2 Outlet | 490.0 | 28.3 | 274.1 | 954 |
| 0312 | PHX1 Inlet | 490.1 | 28.3 | 3749.2 | 954 |
| 0410 | PHX Outlet | 730.0 | 27.6 | 3749.2 | 1259 |
| 0411 | Power Turbine Inlet | 730.0 | 27.6 | 2823.6 | 1259 |
| 0412 | HT Comp Turbine Inlet | 729.9 | 27.6 | 649.6 | 1259 |
| 0413 | LT Comp Turbine Inlet | 729.7 | 27.6 | 276.0 | 1259 |
| 0511 | Power Turbine Outlet | 516.4 | 5.7 | 2823.6 | 1007 |
| 0512 | HT Comp Turbine Outlet | 521.2 | 5.7 | 649.6 | 1012 |
| 0513 | LT Comp Turbine Outlet | 525.2 | 5.7 | 276.0 | 1017 |
| 0514 | HT Comp Turbine + Power Turbine Outlet | 517.1 | 5.7 | 3473.2 | 1008 |
| 0510 | RHX1 LP Inlet | 517.9 | 5.7 | 3749.2 | 1008 |
| 0610 | RHX1 LP Outlet - RHX2 LP Inlet | 213.6 | 5.7 | 3749.2 | 663 |
| 0621 | RHX2 LP Outlet | 48.4 | 5.5 | 3749.2 | 472 |
| 0622 | HT Comp Inlet | 48.4 | 5.5 | 1543.2 | 472 |
| 0623 | ACC Inlet | 48.4 | 5.5 | 2206.0 | 472 |

| SYSTEM PARASITICS | Loss (kW _e) | Power (kW _e) |
|---------------------------|-------------------------|--------------------------|
| Power Turbine Gross Power | - | 713,432 |
| Gearbox/Generator | (3,567) | |
| Component Electrical | (11,553) | |
| Coal Handling | (456) | |
| Pulverizers | (3,818) | |
| Sorbent / Reagent | (144) | |
| Ash Handling | (856) | |
| Primary Air Fans | (1,793) | |
| Forced Draft Fans | (704) | |
| Induced Draft Fans | (5,827) | |
| Main Air Compressor | (75,004) | |
| ASU Aux | (1,000) | |
| Baghouse | (120) | |
| Spray Dryer FGD | (2,329) | |
| CPU | (51,817) | |
| Misc BOP | (2,000) | |
| Turbine Aux | (400) | |
| Transformer Losses | (2,051) | |
| System Net Power | | 549,992 |

| Component | Duty (kW) |
|-----------------------------------|-----------|
| LT Turbo-Compressor - Shaft Power | 66,760 |
| HT Turbo-Compressor - Shaft Power | 160,254 |
| Power Turbine - Shaft Power | 713,422 |
| ACC - Heat Transferred | 531,785 |
| RHX1 - Heat Transferred | 1,294,736 |
| RHX2 - Heat Transferred | 716,096 |
| PHX1 - Heat Transferred | 1,143,113 |
| PHX2 - Heat Transferred | 102,089 |